ISSN 1846-6168 (Print), ISSN 1848-5588 (Online)
https://doi.org/10.31803/tg-20220920172008

Original scientific paper
Received: 2022-09-20, Accepted: 2022-11-02

Unbalance Response Analysis of a Rotor Kit with Two Identical Discs Located Between Bearings

Marko Katinić*, Josip Kolar, Pejo Konjatić, Mladen Bošnjaković

Abstract: In this paper, the dynamic behavior of a rotor kit with two identical disks located between the plain bearings was analyzed. Modal and harmonic analysis of this rotor kit configuration were performed in the Ansys software package. To calibrate the bearing parameters (stiffness and damping) in the numerical model, experimental measurements of the rotor kit with a disc mounted at the midspan of the shaft were performed. As a result of modal analysis, natural frequencies and models were obtained. Using the Campbell's diagram, the critical speeds and the influence of the gyroscopic effects on the natural frequencies were determined. The responses of the rotor kit to different unbalance distributions were considered by harmonic analysis.

Keywords: Campbell diagram; critical speed; harmonic analysis; modal analysis; rotor kit; unbalance

1 INTRODUCTION

The vibration of a rotating machine occurs as a result of dynamic forces. Vibration usually appears as radial (lateral), axial and torsional. Radial vibration causes the most common machine problem, and is therefore commonly measured. Axial vibration occurs only in some special machine operating conditions (for example, compressor surge). Measuring torsional vibration is quite difficult, so this vibration is usually neglected.

Machine vibration causes cyclic stresses in machine components, which can result in high-cycle fatigue failure and forced shutdown of the machine. If the displacements due to vibration are large enough, it can cause unwanted contact between rotating and stationary machine parts, causing wear or damage.

The most common dynamic force that produces radial vibration in rotating machines is unbalance. The non-uniform distribution of the rotor mass during the rotation of the rotor creates a centrifugal force. The rotating centrifugal force has a frequency equal to the rotor speed and causes a synchronous vibration of the rotor. The vibration amplitude increases when the rotor speed approaches the value of the rotor's natural frequency. When the rotor speed becomes equal to the natural frequency, the rotor has reached a balance resonance which is known as the critical speed or critical [1]. At the critical speed, the vibration amplitude reaches its maximum value.

Modern rotating machines, such as gas and steam turbines, centrifugal compressors, have high operating speeds and vibration problems are much more pronounced than for other machines. Some of these machines operate below the first critical, while most fairly large machines in the process industry operate above the first or even more critical speeds. This means that it is important to consider the amplification of rotor vibration in resonance during the start-up or shutdown of the machine. High vibration at resonance results in high rotor stresses, danger of rotor-to-stator contact and wear of seals and bearings [1-3].

Because of the above mentioned, the main areas of consideration in rotary machine design are critical speeds and unbalance response. As a first step in rotor design, an analysis is performed to determine critical speeds and mode shapes. Then the analysis of unbalance response is carried out. This analysis provides an answer as to whether an unbalance response problem can be expected for a particular mode. For this purpose, various commercial software packages (Abaqus, Ansys, etc.) or specialized programs for rotor dynamics (Dynamics R4, MADYN 2000, DeRoBeS, etc.) are used.

To achieve a better understanding of rotor dynamic behaviour, experimental research is often carried out on a rotor kit that is specially designed to simulate behaviour of the actual rotor [4-8]. Investigations of unbalance response were mainly carried out on a single-disc rotor kit. However, most rotors have two or more discs or impellers mounted on the rotor shaft. Therefore, it is of interest to investigate the unbalance response of a rotor kit with two or more discs mounted on a shaft.

In this paper, the dynamic behavior of a rotor kit with two identical discs located between the plain bearings was analyzed. The analysis was performed by the Ansys software package [9]. Bearing parameters used in the numerical model were determined using data obtained from experimental measurements of the response of a rotor kit with a disc mounted at the midspan of the shaft. By modal analysis of a rotor kit with two discs, natural frequencies and mode shapes were obtained. The critical speeds of the rotor kit were determined using Campbell's diagram. Finally, a harmonic analysis was performed to determine the response to unbalance. The responses to different unbalance distributions were considered.

2 MODAL AND HARMONIC ANALYSIS

The analyzed two-disc rotor kit is shown in Fig. 1 [10]. Each rotor disc has 16 threaded holes for mounting M5 screws of different masses. The holes are located equidistantly on a disc radius of 30 mm.

The material of the rotor kit is steel with a density of 7850 kg/m^3. Its modulus of elasticity is 210 GPa and Poisson's ratio is 0.3.

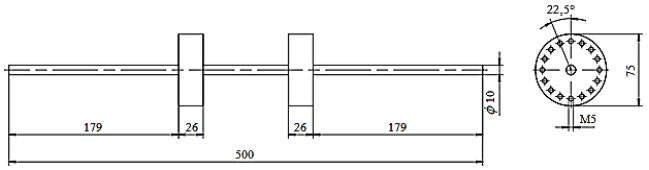

Figure 1 Rotor kit with two discs [10]

The rotor shaft is supported by two plain bearings located at the ends of the shaft. The bearing parameters (stiffness and damping) for the numerical model of the rotor kit were determined experimentally using a rotor kit with a disc located at the midspan of the shaft.

2.1 Determination of Bearing Parameters

The dimensions of the rotor kit with a disc are shown in Fig. 2.

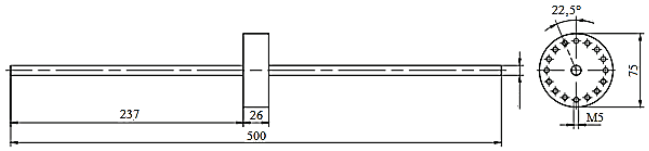

Figure 2 Rotor kit with a disc [10]

Fig. 3 shows the experimental measuring scheme of the rotor kit. Labels *r1x*, *r1y*, *r2x*, *r2y* indicate proximity vibration probes in the *x* and *y* directions for the first and second measuring location, respectively. Bearing stiffness constants in the *x* and *y* directions are denoted by K_{bx} and K_{by}. C_{bx} and C_{by} denote the damping constants of the bearing in the *x* and *y* directions.

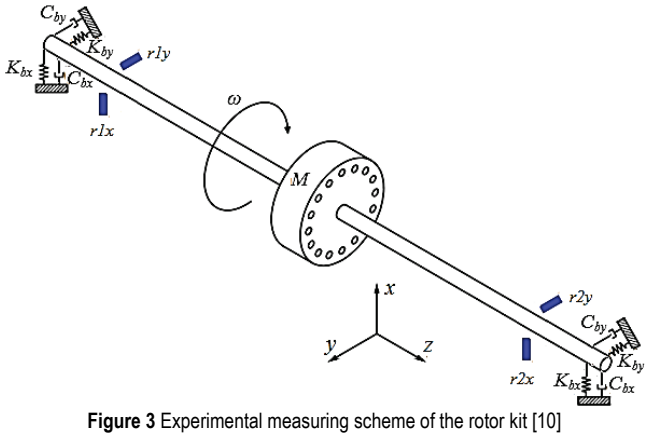

Figure 3 Experimental measuring scheme of the rotor kit [10]

Experimental vibration measurements were performed on the RK4 produced by Bently Nevada [4] (Fig. 4). The measurements were carried out using a specialized system for data acquisition and processing, which is a product of Turbocom company from Croatia. At two measuring points, which are at a distance of 65 mm from the centre of each bearing (to avoid the occurrence of a nodal point), proximity probes of the Bently Nevada system 3300 – 8 mm were installed. These probes measure the peak-to-peak (pp) vibration amplitude in µm. The measurements were carried out in a transient condition, by simulating the start-up of the rotor from 0 rpm to 10000 rpm. The rotor speed was increased by constant angular acceleration.

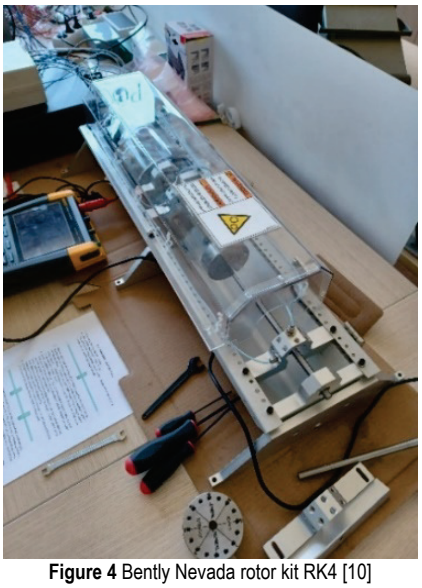

Figure 4 Bently Nevada rotor kit RK4 [10]

Fig. 5 shows the obtained Bode plot of the start-up, which shows the change in amplitude and phase of synchronous vibration (1X) versus rotor speed.

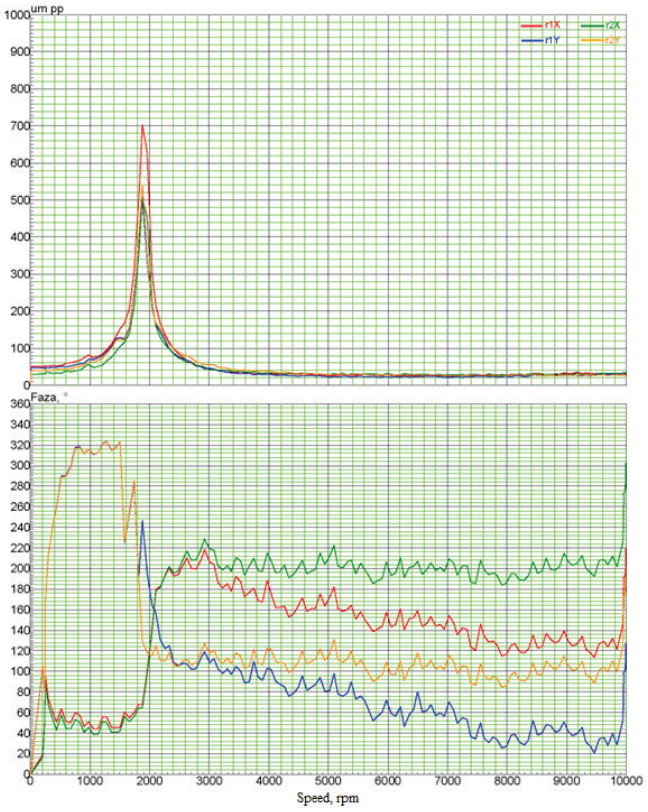

Figure 5 Bode plot [10]

The data from the Bode plot were used to determine the stiffness and damping constants of the bearings. According to [10], the obtained constants are as follows: $K_{bx} = K_{by} = 149$ kN/m and $C_{bx} = C_{by} = 9.445$ Ns/m.

These values of constants were confirmed by the modal analysis of the rotor kit in Ansys software. The geometric model of the rotor-bearing system is shown in Fig. 6, where the bearing model in Ansys is implemented as a mechanical connection type defined at selected locations of the shaft. Bearing modelling using the Bearing Connection option allows defining the stiffness and damping constants of the bearings.

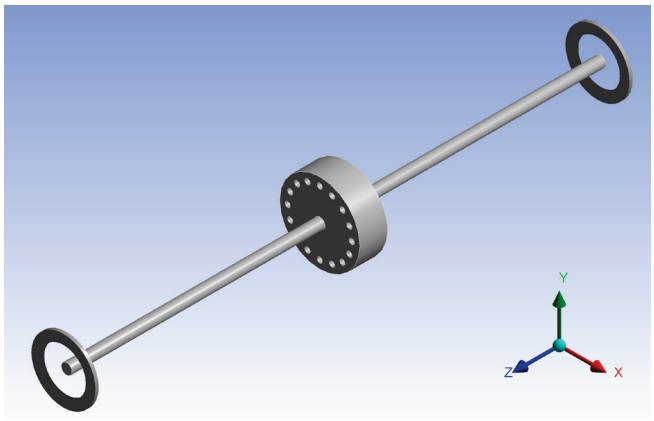

Figure 6 Rotor-bearing system in Ansys [10]

Discretization of the model was performed automatically, with a mesh of finite elements of size 3 mm. The finite element mesh was generated with SOLID 187 finite elements. Fig. 7 shows the meshed model of the rotor kit.

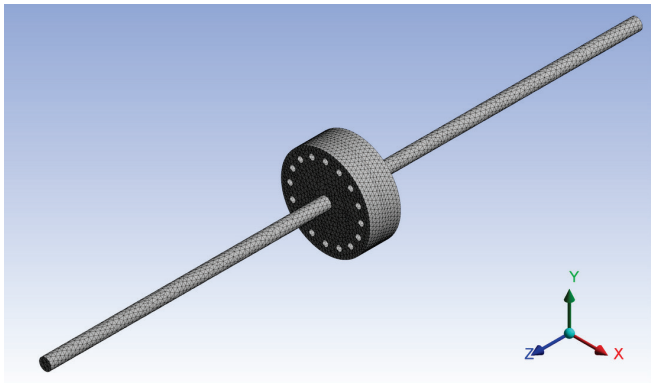

Figure 7 Meshed model of the rotor kit [10]

The boundary conditions are set so that the rotation in relation to the longitudinal axis of the rotor was fixed, and the rotations around the two remaining axes remained free to avoid the so-called "zero pivot" error in the solver. The axial displacement of the rotor is also fixed. The considered rotor speeds from 0 to 10000 rpm with a step of 1000 rpm are defined tabularly in Ansys. In the analysis settings, the first five (5) modes of vibration are defined, and the creation of a Campbell diagram is also included. Natural frequencies are calculated for each considered rotor speed.

Tab. 1 gives the calculated values of the first five natural frequencies for zero rotor speed [10]. Modes 1 and 2 represent the first bending mode with forward (FW) and backward (BW) whirling, respectively. Mode 3 is the first torsional mode, while modes 4 and 5 represent the second bending mode with forward (FW) and backward (BW) whirling, respectively.

Table 1 Natural frequencies of the single-disc rotor kit at zero speed [10]

Mode	Natural frequency, Hz
1	31.66
2	31.67
3	120.67
4	203.85
5	203.85

Fig. 8 shows the Campbell diagram, which is one of the most important engineering tools for determining rotor critical speeds. The diagram shows the dependence of the natural frequencies of the system and the excitation frequencies as a function of the rotor speed. On the abscissa of the diagram is the rotor speed in revolutions per minute (rpm), and on the ordinate is the frequency in Hertz (Hz).

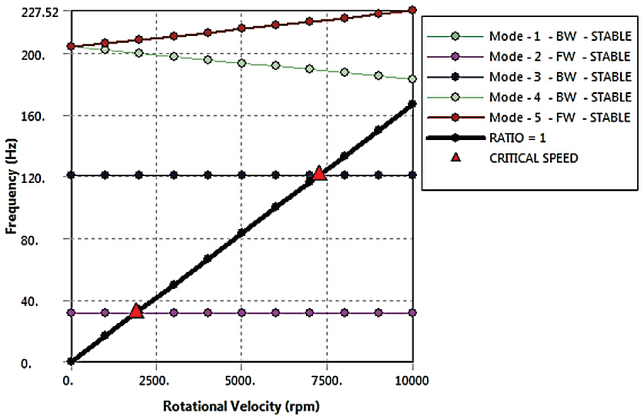

Figure 8 Campbell diagram for the single-disc rotor kit [10]

It is evident from the diagram that the natural frequencies of the first three modes (the first bending with FW and BW and the first torsional) do not change with the rotor speed. This means that there is no influence of the gyroscopic effect on the spring stiffness of the rotor system. However, for the remaining two modes (the second bending with FW and BW), the change of natural frequencies with the rotor speed is obvious. For the second bending mode with FW, the natural frequency increases linearly with increasing rotor speed, which is the result of increasing the stiffness of the system due to the gyroscopic effect. This phenomenon is known as gyroscopic stiffening. On the other hand, for the second bending mode with BW, the natural frequency decreases linearly with increasing rotor speed, which is the result of the reduction of system stiffness due to the gyroscopic effect. This phenomenon is known as gyroscopic softening. In the diagram, one additional straight line can be seen (marked as RATIO = 1), which is called the excitation line. This line corresponds to an excitation with a frequency that coincides with the rotation frequency of the rotor. It is

evident that the excitation line intersects the natural frequency lines of the first bending mode with FW and BW. The point of intersection of these lines determines the critical speed of the rotor, which is 1900 rpm. There is no deviation between the numerically and experimentally determined critical speed. This gives full confidence in the numerical model of the rotor kit. The excitation line also intersects the natural frequency of the first torsional mode, so there is also a torsional critical speed of 7240 rpm.

2.2 Modal Analysis of a Two-Disc Rotor Kit

A modal analysis of the two-disc rotor kit shown in Fig. 2 was performed with the aim of determining the natural frequencies and associated mode shapes. To create a numerical model of the rotor kit, the bearing parameters obtained in chapter 2.1 were used. The geometric model of the rotor-bearing system is shown in Fig. 9.

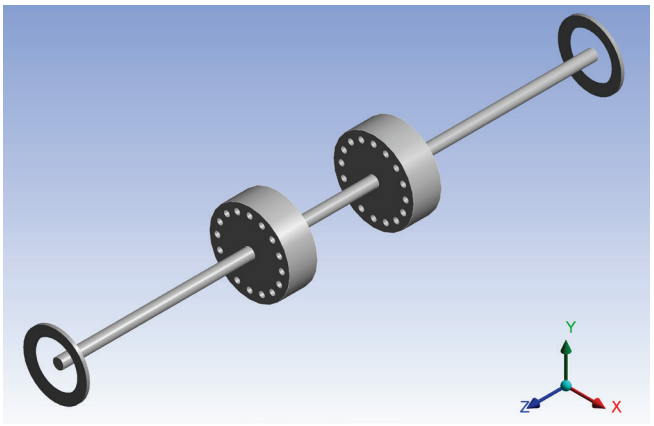

Figure 9 Rotor-bearing system in Ansys [10]

Fig. 10 shows the meshed model of the rotor kit. The finite element mesh was generated automatically using SOLID 187 finite elements of size 3 mm.

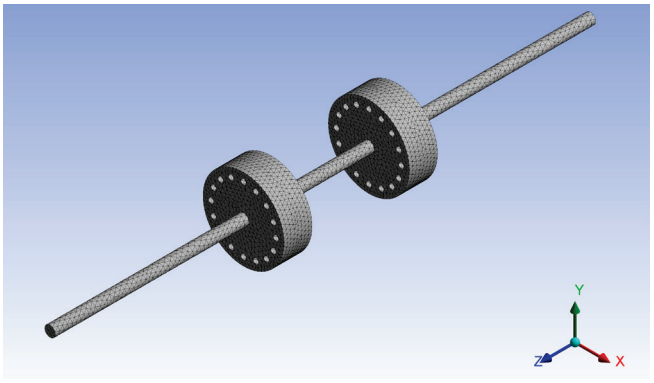

Figure 10 Meshed model of the rotor kit [10]

Identical boundary conditions are set as in the case of single-disc rotors. The considered rotor speeds from 0 to 10000 rpm with a step of 1000 rpm are defined tabularly in Ansys. In the analysis settings, the first 6 modes of vibration are selected. The creation of a Campbell diagram is also included. Natural frequencies are calculated for each considered rotor speed.

The calculated values of natural frequencies for zero rotor speed are given in Tab. 2 [10].

Table 2 Natural frequencies of the two-disc rotor kit at zero speed [10]

Mode	Natural frequency, Hz
1	25.38
2	25.38
3	91.77
4	116.89
5	116.90
6	293.12

The first bending modes with BW and FW are shown in Fig. 11 and Fig. 12, respectively.

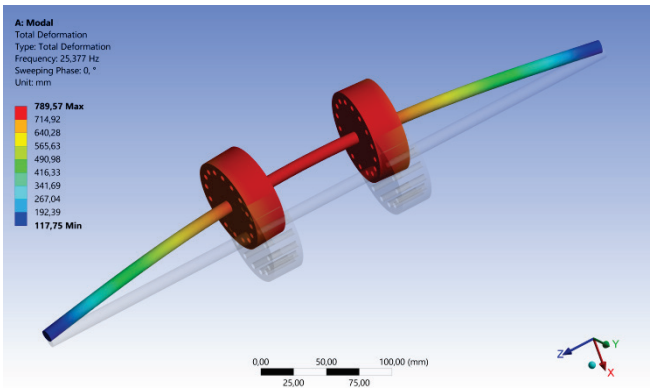

Figure 11 The first bending mode with BW

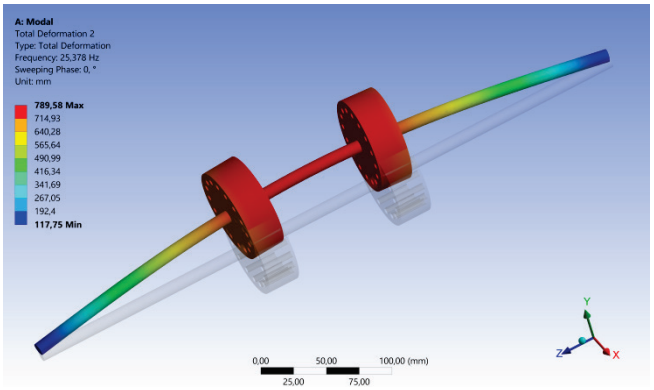

Figure 12 The first bending mode with FW

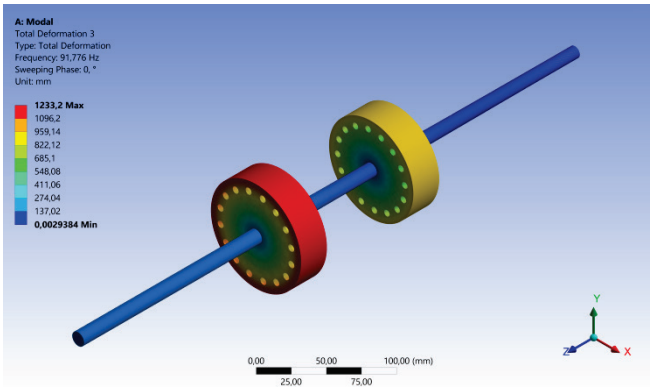

Figure 13 The first torsional mode

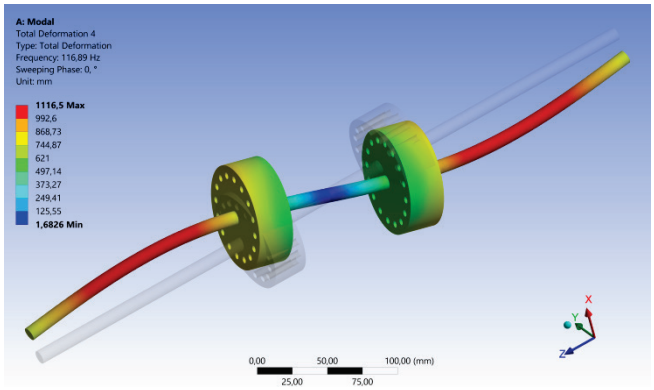

Figure 14 The second bending mode with BW

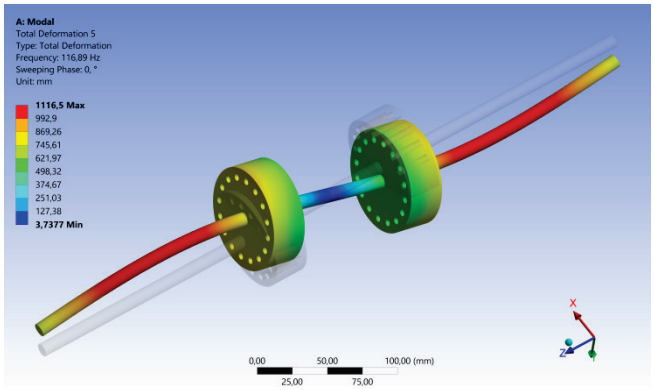

Figure 15 The second bending mode with FW

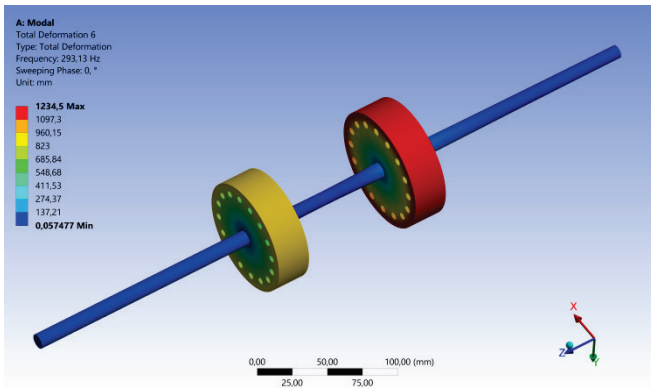

Figure 16 The second torsional mode

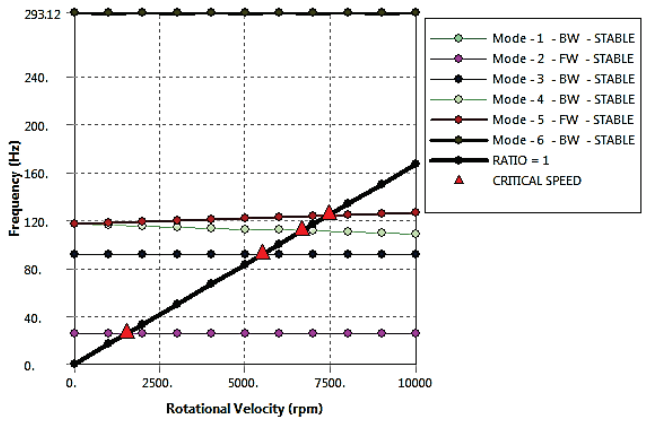

Figure 17 Campbell diagram for the two-disc rotor kit [10]

The first and second torsional modes are shown in Fig. 13 and Fig. 16, respectively.

The second bending modes with BW and FW are shown in Fig. 14 and Fig. 15, respectively.

Campbell diagram is shown in Fig. 17.

It is evident from the diagram that the natural frequencies of the first bending FW and BW, and the first and second torsional modes do not change with the rotor speed. This means that there is no influence of gyroscopic effect on the spring stiffness of the rotor system. However, for the second bending mode with FW and BW, there is a change in natural frequencies with changing rotor speed. For the second bending mode with FW, the natural frequency increases linearly with increasing rotor speed, which is the result of gyroscopic stiffening. On the other hand, for the second bending mode with BW, the natural frequency decreases linearly with increasing rotor speed, which is the result of gyroscopic softening. The excitation line (marked with RATIO = 1) intersects the lines of the first and second bending modes and the first torsional mode. The points of intersection of these lines indicate the critical speeds of the rotor. The intersection point with the natural frequency lines of the first bending mode (FW and BW lines) determines the first critical speed of the rotor, which is 1525 rpm. Since the change of the natural frequency of the second bending mode is affected by the gyroscopic effect, the excitation line intersects the natural frequency lines of this mode (FW and BW lines) at two different points, which represent the second critical speed of the rotor. In the case of FW, the second critical speed is 7436 rpm, and in the case of BW, it is 6656 rpm. Torsional critical speed is 5506 rpm.

2.3 Harmonic Analysis of a Two-Disc Rotor Kit

Actual rotor systems in operation are subjected to forced vibration. Rotating unbalance is the most common form of rotor excitation. The distribution of rotating unbalance creates an axially distributed force system that can excite the natural frequencies. This force system has a form that is conceptually similar to a mode shape. How much a natural mode will be excited depends on the unbalance distribution and how well it matches a particular mode shape. Good unbalance matching results in relatively high mode excitation (a rotor resonance). A poor unbalance match produces little or no mode excitation, and little or no resonance [1].

Using the example of the described rotor kit with two discs (Fig. 1), a harmonic analysis was performed with the aim of determining the influence of different axial distributions of unbalance on the excitation of vibration modes. Unbalance is simulated by adding concentrated masses to the rotor discs at a radius of 30 mm. The analysis was performed using two masses of 0.8 g. Three different harmonic analyses were performed. The first analysis consisted in determining the response of the rotor kit to the in-phase unbalance distribution (Fig. 18). Namely, a mass of 0.8 g was added to each disc and the added masses are in phase (at the same angle). The response of the rotor kit to the out-of-phase unbalance distribution was found in the second analysis (Fig. 19). A mass of 0.8 g is added to each disc, but

the added masses are out-of-phase (the phase difference is 180°). In the third analysis, the response of the rotor kit to the asymmetric distribution of the imbalance, which was achieved by adding a single mass of 0.8 g to only one disc, was investigated. In all analyses, it was chosen that the unbalance has the same direction of rotation as the rotor kit.

The finite element mesh and boundary conditions are identical as in modal analysis. The analysis was performed using the direct integration method [9]. The frequency response was taken on the rotor discs. The selected frequency range for considering the response is 0 to 170 Hz.

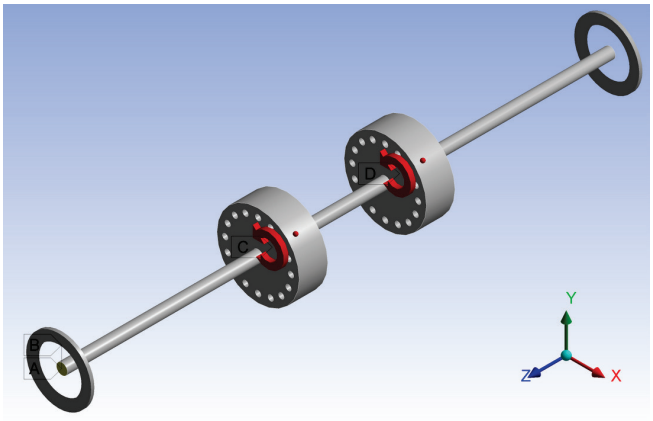

Figure 18 The in-phase unbalance distribution [10]

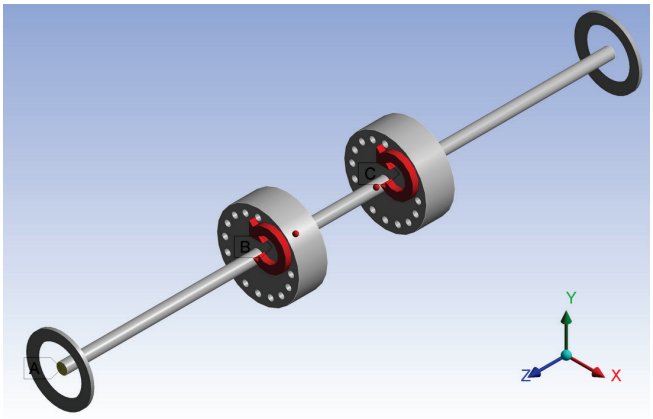

Figure 19 The out-of-phase unbalance distribution [10]

The frequency response is displayed using a Bode plot, which consists of two separate diagrams. The first diagram shows the dependence of the amplitude of the response on the frequency, and the second diagram shows the dependence of the phase of the response on the frequency. Figs. 20 and 21 show the frequency response plots for the *x* and *y* axis, respectively, when the unbalance distribution is in-phase.

The peak of the vibration amplitude at a frequency of 25 Hz is clearly visible on both plots. At this frequency, the phase angle of the response changes by 180°, and the frequency 25 Hz is obviously the resonant frequency. At this frequency, the amplitude is limited only by the damping of the system. From the modal analysis, it is evident that it is the natural frequency of the first bending mode with FW. It means the in-phase unbalance distribution excites only the first mode, because it matches the first mode. The second mode is not excited because the unbalance distribution does not match the second mode shape.

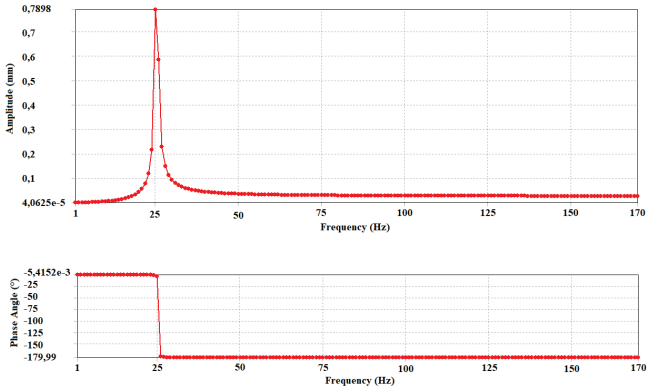

Figure 20 Response to in-phase unbalance distribution for the *x* axis [10]

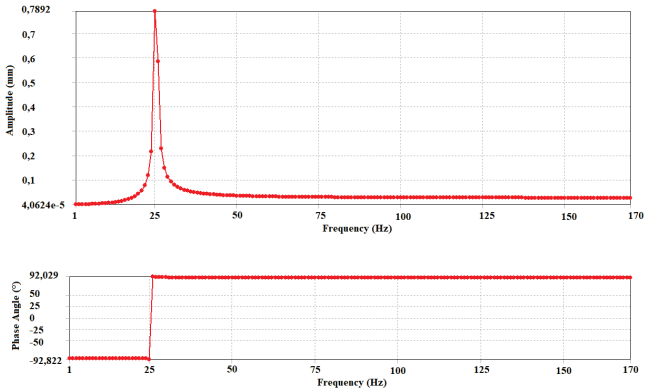

Figure 21 Response to in-phase unbalance distribution for the *y* axis [10]

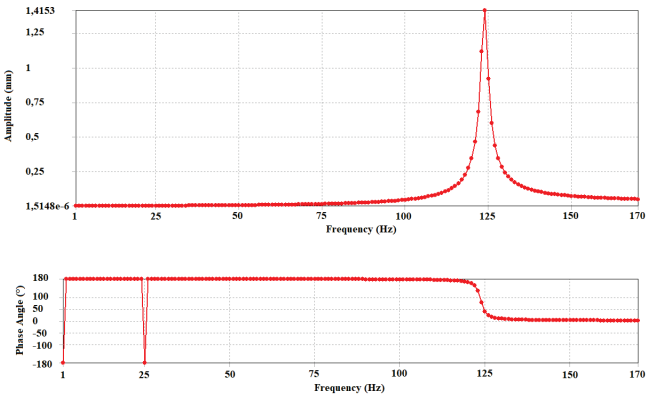

Figure 22 Response to out-of-phase unbalance distribution for the *x* axis [10]

Figs. 22 and 23 show the frequency response plots for the *x* and *y* axis, respectively, when the unbalance distribution is out-of-phase. The peak of the vibration amplitude at a frequency of 124 Hz is clearly visible on both plots. This frequency is obviously the resonant frequency. From the modal analysis, it is evident that it is the natural frequency of the second bending mode with FW. It means the out-of-phase unbalance distribution excites only the second mode. The first mode is not excited because the unbalance distribution does not fit the first mode shape.

In the general case of unbalance distribution (asymmetric unbalance distribution) both bending modes of

vibration are excited. This was confirmed by harmonic analysis which obtained the response of a two-disc rotor for an unbalance mass of 0.8 g added to a 30 mm radius of only one disc. Figs. 24 and 25 show the corresponding frequency responses. The frequency response for *x* axis is shown in Fig. 24, and for the *y* axis in Fig. 25.

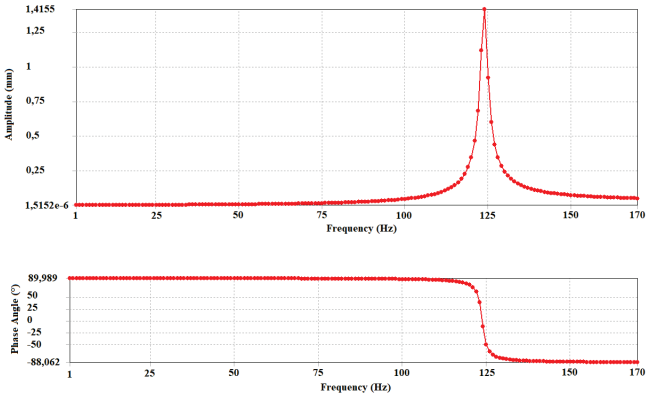

Figure 23 Response to out-of-phase unbalance distribution for the *y* axis [10]

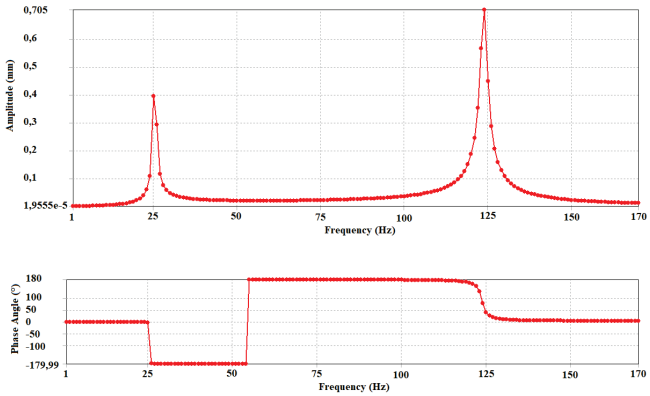

Figure 24 Response to asymmetric unbalance distribution for the *x* axis [10]

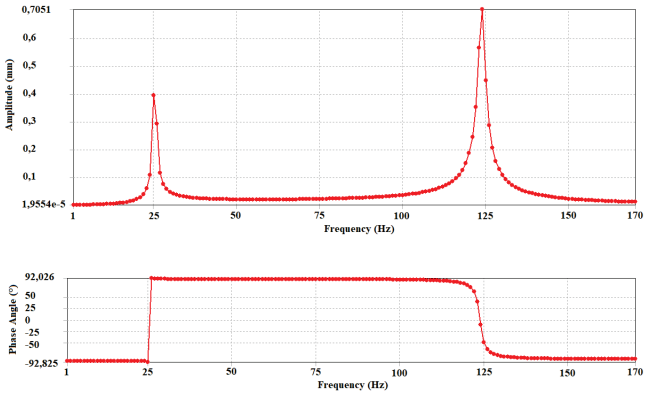

Figure 25 Response to asymmetric unbalance distribution for the *y* axis [10]

As can be clearly seen from both responses, resonant amplitude peaks appear at frequencies of 25 Hz and 124 Hz. In this way, it was proved that the general unbalance, which appears in practical cases, excites both bending modes of vibration.

3 CONCLUSIONS

Modal and harmonic analysis of the two-disc rotor kit was performed. The discs are located between the rotor bearings and at an identical distance from the adjacent bearing. To perform these analyses, a numerical model was created in the Ansys software package. The numerical model was calibrated and verified using the results of experimental measurements on the rotor kit with a disc mounted at the midspan of the rotor shaft.

Natural frequencies, modes and Campbell diagram were obtained by modal analysis. From the Campbell diagram it was concluded that the two-disc rotor kit in the considered speed range has two critical speeds, has the first and second critical speeds for the first and second bending modes, respectively. The first critical speed is the same for both FW and BW of the rotor, because there is no influence of the gyroscopic effect. However, due to the gyroscopic effect, there are two different second critical speeds: a higher value for FW and a lower value for BW of the rotor.

The responses of the two-disc rotor kit to different unbalance distributions were obtained by harmonic analysis. The in-phase unbalance distribution excites only the first mode, because it matches the first mode. The out-of-phase unbalance distribution excites only the second mode, because it fits the second mode. The asymmetric distribution of the unbalance excites both the first and second modes.

4 REFERENCES

[1] Bently, D. E. (2002). *Fundamentals of Rotating Machinery Diagnostics*. Minden, Bently Pressurized Bearing Press

[2] Jacquet-Richardet, G. Torkhani, M., Cartraud, P., Thouverez, F., Nouri-Baranger, T., Herran, M., Gibert, C., Baguet, S., Almeida, P., & Peletan, L. (2013). Rotor to stator contacts in turbomachines. Review and application. *Mechanical Systems and Signal Processing, 40*(2), 401-420. https://doi.org/10.1016/j.ymssp.2013.05.010

[3] Blair, B. J. & Pethybridge, G. (2010). Hydrodynamic Bearing Damage and Remediation of Contributing Factors in Rotating Machinery. *The 9th EDF/Pprime (LMS) Poitiers Workshop "Improvement of Bearing Performance and Evaluation of Adverse Conditions"*, 1-14.

[4] RK4 Rotor Kit, Datasheet, Bently Nevada. Retrieved from https://dam.bakerhughesds.com/m/5af2591c64daec8f/original/RK4-Rotor-Kit-Datasheet-141592-pdf.pdf

[5] Alsaleh, A., Sedighi, H. M., & Ouakad, H. M. (2020). Experimental and theoretical investigations of the lateral vibrations of an unbalanced Jeffcott rotor. *Frontiers of Structural and Civil Engineering, 14*, 1024-1032. https://doi.org/10.1007/s11709-020-0647-y

[6] Tchomeni, B. X. & Alugongo, A. (2019). Experimental diagnosis of multiple faults on a rotor-stator system by fast Fourier transform and wavelet scalogram. *Journal of Vibroengineering, 21*(4), 911-926. https://doi.org/10.21595/jve.2018.19639

[7] Ryu, J. Y. (2020). Diagnostics of Steam Turbine High Vibration from Coupling Failure. *Orbit Newsletter*, Q4. Retrieved from https://dam.bakerhughesds.com/m/6f504c6a0dea307b/original/Q4-2020-KOSPO-RMC-Orbit-Article.pdf?_ga=2.49610852.332631911.1667326481-1286916522.1667326481

[8] Ishibashi, T. & Kawai, T. (2019). Modeling of Rotating Shaft with Partial Rubbing. *Proceedings of the 13th International Modelica Conference*, Regensburg, Germany, 343-352. https://doi.org/10.3384/ecp19157343
[9] Ansys Inc.: ANSYS 17.2
[10] Kolar, J. (2022). Analysis of rotor dynamics for simulation of dynamic behaviour of rotary machines. *Graduate Thesis.* Mechanical Engineering Faculty in Slavonski Brod (in Croatian)
[11] http://www.turbocom.hr/

Authors' contacts:

Marko Katinić, PhD, Associate Professor
(Corresponding author)
Mechanical Engineering Faculty, University of Slavonski Brod,
Trg I. B. Mažuranić 2, 35000 Slavonski Brod, Croatia
035/493417, mkatinic@unisb.hr

Josip Kolar, Mag. Ing. Mech.
Mechanical Engineering Faculty, University of Slavonski Brod,
Trg I. B. Mažuranić 2, 35000 Slavonski Brod, Croatia
0958948995, jkolar@unisb.hr

Pejo Konjatić, PhD, Full Professor
Mechanical Engineering Faculty, University of Slavonski Brod,
Trg I. B. Mažuranić 2, 35000 Slavonski Brod, Croatia
035/493424, pkonjatic@unisb.hr

Mladen Bošnjaković, PhD, Assistant Professor
Technical Department, University of Slavonski Brod,
Trg I. B. Mažuranić 2, 35000 Slavonski Brod, Croatia
035/492634, mbosnjakovic@unisb.hr